

# All-optical switching in an asymmetric silicon Fabry–Perot étalon based on the free-carrier plasma effect

Y. M. Liu, X. Xiao, P. R. Prucnal, and J. C. Sturm

We demonstrate all-optical switching at 1.3 and 1.5  $\mu\text{m}$  in the reflection mode of an asymmetric silicon Fabry–Perot étalon by a control beam at 0.85  $\mu\text{m}$ . Both switch-on and switch-off operations are demonstrated at different locations of the étalon. Based on the free-carrier plasma effect, a modulation depth as large as 10% is obtained and a frequency response as high as 0.5 GHz is achieved.

So far, silicon (Si) electronics has been the most effective and mature technology for the present semiconductor industry. However, electrical interconnect-based communication between different Si VLSI chips has been a bottleneck at high data rates. It appears that optical interconnects will have a great effect on Si VLSI in the near future by providing a large bandwidth–distance product and immunity from cross talk.<sup>1,2</sup> Optical interconnection requires the integration of some optoelectronic components, such as waveguides, transmitters, and receivers, on Si chips. Heteroepitaxial growth of III–V optoelectronic devices on a Si wafer is one of the possible choices for hybrid integration of optical input–output with Si integrated circuits (IC's). However, the large lattice mismatch ( $\sim 4\%$ ) between Si and III–V elements imposes difficulty in device fabrications. Therefore the natural choice would be developing Si optical devices so that optoelectronic integration is compatible with the present Si processing technology. This monolithic integration technology may offer simpler manufacturing and lower costs than hybrid integration. However, because of its indirect band gap, Si has unfavorable optical properties. Recently there has been an increasing interest in exploring the

optical characteristics of Si. SiGe quantum structures and porous Si may provide an alternative for Si light-emitting devices. GeSi/Si optical waveguides have shown a low-loss characteristic over the communication wavelengths ranging from 1.3 to 1.6  $\mu\text{m}$ .<sup>3,4</sup> Silicon electro-optic modulators, based on the free-carrier effect, have also been demonstrated either in a vertical fiber coupling configuration<sup>5</sup> or in a waveguide Mach–Zehnder configuration.<sup>6</sup> In addition, high-gain GeSi/Si superlattice photodetectors have been demonstrated at 1.3  $\mu\text{m}$ .<sup>7</sup> In this research we study the free-carrier plasma effect in Si for optical devices and demonstrate all-optical switching at 1.3 and 1.5  $\mu\text{m}$  in an asymmetrical silicon Fabry–Perot étalon, by a control beam at 0.85  $\mu\text{m}$ .

Fabry–Perot étalons can perform optical switching and modulation.<sup>8</sup> The principle of such operations is the sweeping of the cavity transmission (or reflection) peak in response to control pulses. If the media inside the cavity is absorptive to the control pulses, the refractive index at the signal wavelength will be changed. As a result, the transmission (or reflection) peak can be shifted to a different state by the control pulses. For example, if the Fabry–Perot transmission peak is initially tuned to the signal wavelength, a switch-on operation occurs in the reflected light if the control pulse shifts the transmission peak and consequently increases the reflectivity of the cavity. For a high-finesse Fabry–Perot cavity, a small change in the intracavity refractive index can translate into a large change in the cavity reflectivity and transmissivity. In our device we use the free-carrier plasma effect caused by the injected free carriers in Si by a control beam at 0.85  $\mu\text{m}$  to reduce the refractive index of the signal beam in the wavelength range of 1.3 to 1.6  $\mu\text{m}$ . As a result, the signal

When this research was performed the authors were with the Advanced Technology Center for Photonics and Optoelectronic Materials, Department of Electrical Engineering, Princeton University, Princeton, New Jersey 08544. Y. M. Liu is now with Opto-Electronics Research, Corning, Inc., SP FR17, Corning, New York 14831.

Received 26 July 1993; revised manuscript received 29 November 1993.

0003-6935/94/183871-04\$06.00/0.

© 1994 Optical Society of America.

beam reflected from the Fabry–Perot cavity will be modulated by the control pulses, and the device response is determined by the temporal and spatial behaviors of the injected carriers.

The étalon consists of a Fabry–Perot resonant cavity formed by a 6.4- $\mu\text{m}$ -thick crystalline Si p-i-n diode sandwiched between two  $\text{SiO}_2$  layers, as shown in Fig. 1. We fabricate the device by epitaxially growing (using chemical vapor deposition) a p-i-n diode on a separation by implantation of oxygen (SIMOX) wafer, which we fabricate by implanting  $\text{O}_2$  into a Si wafer and annealing, forming a 0.2- $\mu\text{m}$  thick buried  $\text{SiO}_2$  layer while still preserving the crystallinity of the cap Si layer. Because  $\text{SiO}_2$  and Si have refractive indices of 1.46 and 3.5, respectively, the buried 0.2- $\mu\text{m}$   $\text{SiO}_2$  layer and the surrounding Si form a multilayer mirror, which has a reflectivity of  $\sim 50\%$  at wavelengths of 1.3–1.6  $\mu\text{m}$ . The Si p-i-n diode is made of a 1.2- $\mu\text{m}$  heavily doped ( $1.1 \times 10^{19}/\text{cm}^3$ ) n<sup>+</sup>-type epitaxial layer, a 4.4- $\mu\text{m}$  lightly doped ( $1.0 \times 10^{16}/\text{cm}^3$ ) n-type layer, and a 0.8- $\mu\text{m}$  heavily doped ( $1.2 \times 10^{20}/\text{cm}^3$ ) p<sup>+</sup>-type layer. After the Si diode is grown a top oxide layer is thermally grown for 0.22  $\mu\text{m}$ , and then 0.10- $\mu\text{m}$  polysilicon is evaporated and annealed as a way to form the top mirror, which is transparent to the control beam at 0.85  $\mu\text{m}$  and highly reflective (80%) at signal wavelengths ranging from 1.3 to 1.6  $\mu\text{m}$ . The device was initially mesa defined for electro-optic intensity modulation at 1.3  $\mu\text{m}$ ,<sup>9</sup> where 40-MHz modulation was obtained with 10% modulation depth. However, the p-i-n diode can be replaced by an intrinsic region in our experiment for all-optical switching.

To confirm the spectral response of the Fabry–Perot cavity, we measure the transmission characteristic with an interferometric spectrophotometer. Figure 2 shows the transmittance versus the wave number; Fig. 2(a) shows an ideal Fabry–Perot étalon with 50% and 80% end mirrors, where the cavity finesse is 7, and Fig. 2(b) shows the experimentally measured Fabry–Perot étalon transmission as a function of the wave number, where the effective finesse is 3. The measured low finesse of the cavity is due to the low reflection of the Si– $\text{SiO}_2$ –Si mirrors with gradual interfaces and the nonuniform thickness of the cavity over the area ( $\sim 3$  mm in diameter) through which the transmittance is measured. However, the

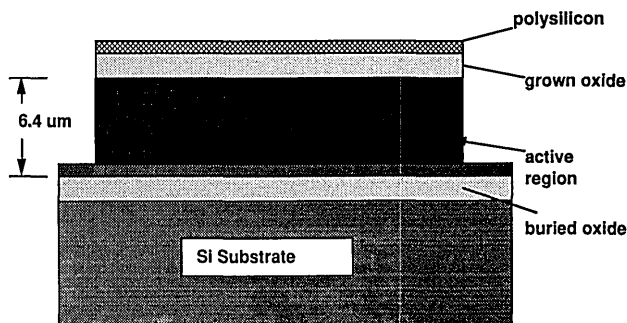


Fig. 1. Cross section of the asymmetric Si Fabry–Perot étalon.

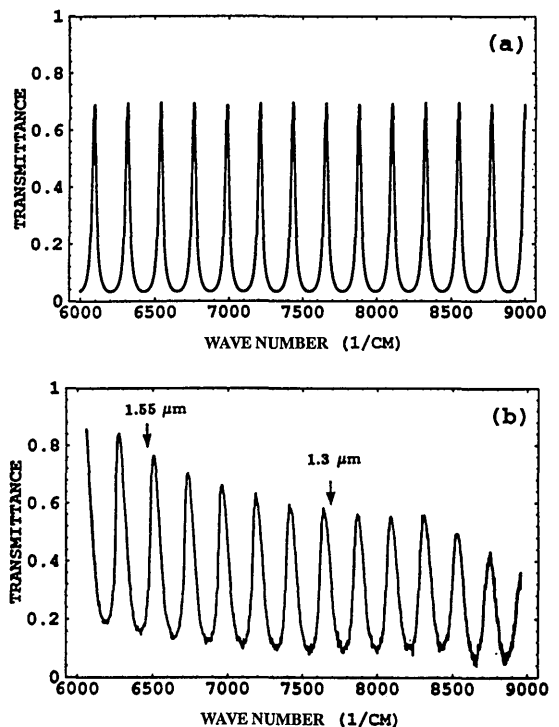


Fig. 2. Transmission characteristic of the Fabry–Perot cavity versus the wave number: (a) theoretical, (b) experimentally measured.

resonant characteristic of the cavity is good for a very large spectral range (1.1–3.0  $\mu\text{m}$ ). In addition, the free spectral range and the passband are 37 and 12 nm, respectively.

The experimental setup for all-optical switching is shown in Fig. 3, in which the control beam is a 100-fs pulse train at 0.85  $\mu\text{m}$  from a self-mode-locked Ti:sapphire laser with a repetition rate of 92 MHz and an average power of 320 mW. The signal beam is from a cw InGaAsP laser diode at 1.5  $\mu\text{m}$ . We focus the control and signal beams to approximately 20  $\mu\text{m}$  in diameter by using a 10 $\times$  microscope objective; the focusing of the signal beam is controlled by another lens so that maximum overlap with the control beam is obtained. The control and modulated signal beams are shown in Fig. 4. The control-pulse duration and signal-beam turn-on time are limited by the response of the detectors used. Trace (a) shows the control beam at 0.85  $\mu\text{m}$ , detected by a Si diode with a

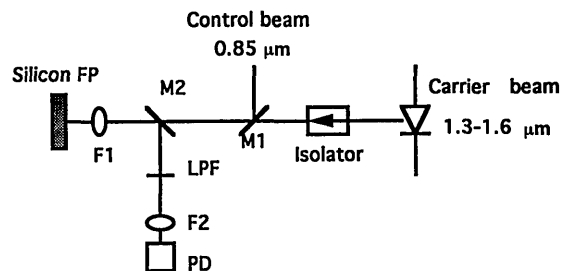


Fig. 3. Experimental setup for all-optical switching: FP, Fabry–Perot étalon; M's, mirrors; F's, focusing lenses; LPF, long-pass filter; PD, photodetector.

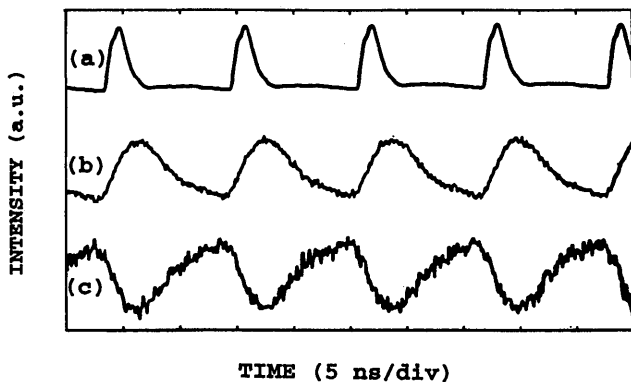


Fig. 4. All-optical switching of a cw 1.5- $\mu\text{m}$  signal beam by 0.85- $\mu\text{m}$  100-fs control pulses at a repetition rate of 92 MHz. Both the signal and control beams are focused to  $\sim 20 \mu\text{m}$  in diameter. (a) Control pulse train, (b) switch on of the signal beam from low reflection to high reflection, (c) switch off of the signal beam from high reflection to low reflection.

response time of  $\sim 1 \text{ ns}$ . Trace (b) shows the modulated signal beam at 1.5  $\mu\text{m}$  with a long recovery time (the detector has a response time of 2 ns). Because the Fabry-Perot cavity is not exactly flat at the edge of the wafer, where the cavity thickness changes  $\sim 1 \mu\text{m}$  for wafer positions 1 cm apart, one can scan the reflectance by moving the wafer transversely. Trace (c) shows the rapid switch off of the signal beam by the control pulse. (Similar results are obtained for signal beams at 1.3  $\mu\text{m}$ .)

Furthermore, we use a laser diode lens to focus both the signal and control beams down to  $\sim 5 \mu\text{m}$  in diameter; a 2-ns recovery time is observed as shown in Fig. 5. Because the modulator employs the free-carrier effect, the device response is determined by the temporal and spatial behaviors of the injected carriers, which are governed by the carrier diffusion and recombination. The response can be improved by a decrease in the long minority-carrier recombination time (lifetime) or by acceleration of the ambipolar carrier diffusion out of the interaction region. Although the carrier lifetime is of the order of 20 ns<sup>6</sup> for Si, our device has a response of 2 ns as a result of the fast transverse diffusion of free carriers out of the interaction region, because smaller dimension and higher carrier density lead to quicker carrier recombination and diffusion. In addition, one can increase the device response further to several gigahertz by

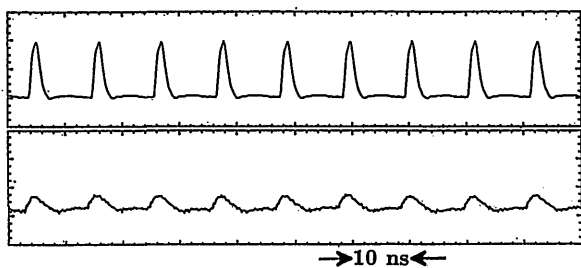


Fig. 5. Switch on of the signal beam at 1.5  $\mu\text{m}$  with a 2-ns recovery time. Both the signal (upper trace) and the control (lower trace) beams are focused to  $\sim 5 \mu\text{m}$  in diameter.

doping lifetime-reducing impurities, such as Au into Si,<sup>10,11</sup> to decrease the minority-carrier lifetime.

In addition, we also measure the modulation depth of the device. For a control-pulse energy of 1.4 nJ and a 20- $\mu\text{m}$  focused spot, the modulation depth is  $\sim 10\%$ . We optimize this by translating the device perpendicular to the focused signal beam so that the device is operated at the maximum slope change regime in the reflection mode for the signal wavelength. For the control pulse of 1.4 nJ, a spot 20  $\mu\text{m}$  in diameter, and with a wavelength of 0.85  $\mu\text{m}$ , the absorption constant for Si is 1050  $\text{cm}^{-1}$  and the injected carrier density is  $2.0 \times 10^{18} \text{ cm}^{-3}$ . Such a high free-carrier density will change the refractive index by 0.0052, which we estimated by using the free-carrier effect data reported in Si.<sup>12</sup> As a result, a maximum reflection change of 15% is calculated in the maximum slope change regime of measured spectral response, as shown in Fig. 2(b). However, the modulation depth could be increased by use of a Fabry-Perot étalon with higher reflectance mirrors.

The thermal stability of the device is also analyzed according to the thermo-optical properties of the crystalline Si. The phase of the Fabry-Perot étalon is affected by temperature through the refractive index  $n$ ; thus its variation is given by  $\delta\phi = (2\pi l/\lambda)\delta n$ , where  $\delta n = (\delta n/\delta T)\Delta T$  is the variation of  $n$  caused by the thermo-optic effect ( $\delta n/\delta T = 1.86 \times 10^{-4} \text{ K}^{-1}$  for Si at 1.5  $\mu\text{m}$ <sup>13</sup>). For a phase shift of  $\pi/6$ , which we find necessary to shift a quarter of the passband of our Fabry-Perot étalon, a temperature change of 97 K is needed, which is much larger than the temperature variation of the surrounding area. Therefore such a device is thermally stable over a large range of temperature variation.

In conclusion, we have demonstrated all-optical switching at 1.3 and 1.5  $\mu\text{m}$  in the reflection mode of an asymmetric Si Fabry-Perot étalon by a control beam at 0.85  $\mu\text{m}$ . We have demonstrated both switch-on and switch-off operations by transversely moving the étalon. Using the free-carrier plasma effect, we have demonstrated a modulation as deep as 10% with a recovery time of  $\sim 2 \text{ ns}$ . The étalon has a spectral range of 37 nm and a passband of 12 nm, and it is applicable over a large spectral range (1–3  $\mu\text{m}$ ).

## References

1. P. R. Prucnal, "Optical interconnects for VLSI local area networks," *IEEE Electrotechnol. Rev.* **2**, 97–98 (1986).
2. P. R. Prucnal, "VLSI optical interconnect networks," in *Integration and Packaging of Optoelectronic Devices*, D. H. Hartman, R. L. Holman, and P. P. Skinner, eds., *Proc. Soc. Photo-Opt. Instrum. Eng.* **703**, 106–115 (1986).
3. S. F. Pesarcik, G. V. Treyz, S. S. Iyer, and J. M. Halbout, "Silicon germanium optical waveguides with 0.5 dB/cm losses for single-mode fiber optic systems," *Electron. Lett.* **28**, 159–160 (1992).
4. Y. M. Liu and P. R. Prucnal, "Deeply-etched single-mode GeSi rib waveguides for silicon-based optoelectronic integration," *Electron. Lett.* **28**, 1434–1435 (1992).
5. B. R. Hemenway, O. Solgaard, A. A. Godil, and D. M. Bloom,

- "A polarization-independent silicon light intensity modulator for 1.32  $\mu\text{m}$  fiber optics," *IEEE Photon. Technol. Lett.* **2**, 262–264 (1990).
6. G. V. Treyz, P. G. May, and J. M. Halbout, "Silicon Mach-Zehnder waveguide interferometers based on the plasma dispersion effect," *Appl. Phys. Lett.* **59**, 771–773 (1991).
  7. T. P. Pearsall, E. A. Bean, H. Temkin, and J. C. Bean, "Ge-Si/Si infra-red, zone-folded superlattice detectors," *Electron. Lett.* **24**, 685–687 (1988).
  8. H. M. Gibbs, T. N. C. Venkatesan, S. L. McCall, A. Passner, A. C. Gossard, and W. Wiegmann, "Optical modulation by optical tuning of a cavity," *Appl. Phys. Lett.* **34**, 511–514 (1979).
  9. X. Xiao, J. C. Sturm, K. K. Goel, and P. V. Schwartz, "Fabry-Perot optical intensity modulator at 1.3  $\mu\text{m}$  in silicon," *IEEE Photon. Technol. Lett.* **3**, 230–231 (1991).
  10. R. Normandin, D. C. Houghton, M. Simard-Normandin, and Y. Zhang, "All-optical silicon-based integrated fiber-optic modulator, logic gate, and self-limiter," *Can. J. Phys.* **66**, 833–840 (1988).
  11. W. M. Bullis, "Properties of gold in silicon," *Solid-State Electron.* **9**, 143–168 (1966).
  12. R. A. Soref and B. R. Bennett, "Electrooptical effects in silicon," *IEEE J. Quantum Electron.* **QE-23**, 123–129 (1987).
  13. G. Cocorullo and I. Rendina, "Thermo-optical modulation at 1.5  $\mu\text{m}$  in a silicon etalon," *Electron. Lett.* **28**, 83–85 (1992).